Coupled in-line and cross-flow vortex-induced vibration responses of a fluid-conveying riser

Zhenhua Li[1], Yangye He[2], Chengbin Liu[3], Yujin Yuan[3], Junfeng Zhao[3], Jian Su[1]

[1]*Nuclear Engineering Department,COPPE, Universidade Federal do Rio de Janeiro*
Centro de Tecnologia, Bloco I, Sala 214, 21941-909, Rio de Janeiro, Brazil
zhenhua.li@lasme.coppe.ufrj.br, sujian@coppe.ufrj.br
[2]*College of Safety and Ocean Engineering, China University of Petroleum-Beijing*
China University of Petroleum-Beijing, 102249, Beijing, China
yangyehe@cup.edu.cn
[3]*CNODC Brasil Petróleo e Gás Ltda, Rio de Janeiro, Brazil*

Abstract. Vortex-induced vibration (VIV) is a significant concern for riser systems, when seawater flows around a riser, it induces vibrations in two primary modes: in-line (IL) and cross-flow (CF). Accurate prediction of the coupled IL and CF VIV behaviors is essential for the structural integrity and design of risers. In this work, the dynamics of a variable-tension fluid-conveying riser under linear shear flow have been studied. The fluid-conveying riser is modeled as a three-dimensional Euler-Bernoulli beam, accounting for variable tension. The hydrodynamic effects impacting the riser are captured by employing two wake oscillators. The generalized integral transform technique (GITT) is applied to transform the coupled system of nonlinear partial differential equations into a system of nonlinear ordinary differential equations. The model was validated by comparing numerical results with experimental data, followed by an in-depth analysis of the internal flow effects on the coupled IL and CF VIV responses. The results reveal that both internal and external flow velocities considerably influence the coupled IL and CF VIV responses of the riser, and an optimal ratio between internal and external flow velocities exists that stabilizes riser vibrations.

Keywords: Vertical riser, Vortex-induced vibration, Coupled IL and CF, Wake oscillator model, Integral transforms

1 Introduction

Riser systems are crucial structural components in offshore oil and gas production, serving as essential connections between subsea installations and surface platforms. Vortex-induced vibration (VIV) emerges as a significant concern for riser systems owing to its complex interactions between the fluid and the structure that affect the structural integrity and lifespan. The VIV responses are predominantly more pronounced in the cross-flow (CF) direction than in the inline (IL) direction, prompting most researchers to concentrate on CF dynamics. However, the behavior of VIV demonstrates coupling effects between these directions, with studies indicating that frequencies in the IL direction are typically twice those in the CF direction[1]. Consequently, the IL responses play a critical role as well. Accurate prediction of VIV is imperative to ensure riser durability and prolong their operational lifespan, constituting a fundamental aspect of safety management in offshore engineering. Thus, exhaustive research into the characteristics of the coupled CF and IL VIV responses, is crucial for enhancing the safety of offshore operations.

In recent years, an increasing number of scholars have focused on research into the coupled VIV dynamics between IL and CF directions. Gu et al.[2] analyzed the nonlinear dynamics of IL and CF VIV, employing a finite difference method alongside a wake oscillator model that accounted for variations in mean top tension. Jiang et al.[3] investigated the impact of cross flow on the coupled CF and IL VIV responses of a flexible fluid-conveying riser with supported ends, utilizing the Galerkin method. Gao et al.[4] developed a three-dimensional time-domain coupled model incorporating variations in added mass coefficients for both IL and CF directions, employing the finite element method to assess how top tension, seawater flow speed, and platform motion influence the riser. Opinel and Srinil[5] presented a nonlinear time-domain simulation model for predicting the two-dimensional VIV of a flexibly mounted circular cylinder in planar and oscillatory flow. It can be concluded from these investigations that the calculation results were more accurate after considering the coupling effect of IL and CF responses.

Two primary numerical methods are widely employed to simulate structural and flow interactions. One is the computational fluid dynamics (CFD), despite its growing effectiveness in predicting VIV dynamics, is still limited by substantial computational requirements. The other, a semi-empirical method, precisely models the principal characteristics of VIV observed in experimental settings by empirically quantifying fluid forces. The concept of a diffusive wake oscillator, first proposed by Mike Gaster[6], was to interpret experimental results of vortex shedding from slender cones at low Reynolds numbers. Skop and Balasubramanian[7] obtained quantitative agreement between the predictions of the diffusive van der Pol oscillator and experimental data in linear shear flow. Facchinetti[8] demonstrated that the diffusive interaction along the continuously distributed van der Pol oscillators could model cellular vortex shedding in shear flow. Mathelin and De Langre[9] used a distribution of nonlinear van der Pol oscillators with diffusion to model rigid and flexible cables.

The effects of internal fluid transported by the riser have also been receiving increasing attention. Zhang et al.[10] investigated the VIV of a fluid-conveying marine riser under the action of harmonically varying tension using the finite element method. The Generalized Integral Transform Technique (GITT) has been extensively utilized to address fluid-structure interaction and VIV problems [11]. This work, for the first time, combines double van der Pol wake oscillators with the GITT to analyze the coupled IL and CF VIV in a top-tensioned vertical riser conveying internal fluid under linear shear flow conditions. The system of nonlinear partial differential equations is integral transformed into a set of nonlinear ordinary differential equations in time, allowing for numerical solutions using established algorithms. The study systematically investigates the effects of the coupled CF and IL VIV of the riser.

2 Mathematical mode

The VIV of a vertical riser in a linear shear flow with its length L, inner diameter d, and outer diameter D, as illustrated in Fig. 1 (a). The bending stiffness of the riser is EI. The riser contains a single-phase fluid (oil or water) with a constant velocity U_i. It is assumed to have simply-supported ends, and utilizes a Cartesian coordinate system, where the x-axis aligns with the current direction, the z-axis opposes gravity, and the y-axis is perpendicular to the xz-plane.

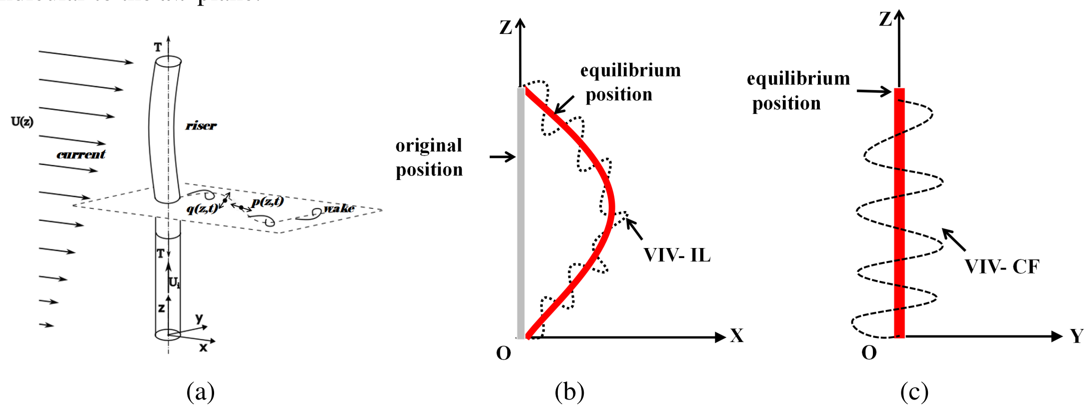

Figure 1. Responses of a fluid-conveying vertical riser in a linear shear flow: (a) illustration of the riser; (b) VIV in IL direction; (c) VIV in CF direction

The mean drag force experienced by the riser in the IL direction leads to a displacement known as the initial bending, positioning the riser in what is termed the equilibrium position, as depicted in Fig.1(b). As the fluid moves past the riser, vortex formation occurs, leading to periodic shedding. This shedding process generates periodic vortex-induced forces across both the CF and IL planes, resulting in vibrations known as VIV, as shown in Fig.1(b) and (c).

2.1 Governing equation of vibration

We consider that the riser vibrates bidirectionally, with the in-line defection $u(z, t)$ and transverse deflection $v(z, t)$ governing by the following equations of motion [12]:

$$m\frac{\partial^2 u}{\partial t^2} + m_f U_i^2 \frac{\partial^2 u}{\partial z^2} + 2m_f U_i \frac{\partial^2 u}{\partial z \partial t} + C_s \frac{\partial u}{\partial t} - \frac{\partial}{\partial z}\left(T(z,t)\frac{\partial u}{\partial z}\right) + EI\frac{\partial^4 u}{\partial z^4} = F_x(z,t) \tag{1}$$

$$m\frac{\partial^2 v}{\partial t^2} + m_f U_i^2 \frac{\partial^2 v}{\partial z^2} + 2m_f U_i \frac{\partial^2 v}{\partial z \partial t} + C_s \frac{\partial v}{\partial t} - \frac{\partial}{\partial z}\left(T(z,t)\frac{\partial v}{\partial z}\right) + EI\frac{\partial^4 v}{\partial z^4} = F_y(z,t) \tag{2}$$

where t is the time, C_s is the structural damping coefficient, and the total mass is $m = m_s + m_f + m_a$. The riser structural material m_s, internal fluid mass m_f, and external fluid-added mass m_a per unit length are $m_s = \rho_s A_s = \frac{\pi}{4}\rho_s(D^2 - d^2)$, $m_f = \rho_f A_f = \frac{\pi}{4}\rho_s d^2$ and $m_a = C_M \frac{\pi}{4}\rho_w D^2$, where ρ_s, ρ_f, and ρ_w are respectively the density of the structural material, inner fluid, and the sea water, A_s is the transversal area of the riser structure, A_f is the inner fluid area, and C_M is the added mass coefficient. The variable tension along the riser length is, $T(z,t) = T_{\text{top}} - (L-z)W_r + \Delta T(z,t)$, the wet weight per unit length of the riser W_r is, $W_r = \left(\frac{\pi}{4}\rho_s(D^2 - d^2) + \frac{\pi}{4}\rho_f d^2 - \frac{\pi}{4}\rho_w D^2\right) g$. The incremental tension is $\Delta T(z,t) = EA_s\frac{S-L}{L}$, and the stretched total length is $S = L + \frac{1}{2}\int_0^L \left(\frac{\partial u}{\partial z}\right)^2 + \left(\frac{\partial v}{\partial z}\right)^2 \, \mathrm{d}z$.

2.2 The hydrodynamic forces

The total hydrodynamic force on the riser each unit length is given by:

$$\vec{F} = \vec{F}_L + \vec{F}_D, \tag{3}$$

where the lift force $\vec{F}_L$ and the drag force $\vec{F}_D$ are related to the velocity vector $\vec{U}_R = \vec{U} - \vec{V}$ between the external speed $\vec{U}$ and the riser speed $\vec{V}$,

$$\vec{F_D} = \frac{1}{2}\rho_w C_D D|\vec{U}_R|\vec{U}_R, \tag{4}$$

$$\vec{F_L} = \frac{1}{2}\rho_w C_L D|\vec{U}_R|\mathbf{R}\cdot\vec{U}_R, \tag{5}$$

where $\mathbf{R}$ is a tensor of rotation. C_D and C_L are the drag and lift coefficients.

2.3 Coupling with double wake oscillators

The drag coefficient C_D is decomposed as a constant mean drag and a fluctuating part, which is related to the vortex shedding[13],

$$C_D = C_{DM} + C_{Df}. \tag{6}$$

The drag and lift coefficients are related to the coefficient $p(z,t)$ and $q(z,t)$ respectively by,

$$C_{Df}(z,t) = \frac{C_{D0}}{2}p(z,t), \tag{7}$$

$$C_L(z,t) = \frac{C_{L0}}{2}q(z,t). \tag{8}$$

in which C_{D0}, C_{L0} are the amplitude.

The reduced lift and drag coefficients $q(z,t)$ and $p(z,t)$ are governed by a double diffusive wake oscillator model ,

$$\frac{\partial^2 q}{\partial t^2} + \epsilon\Omega_f(z)(q^2-1)\frac{\partial q}{\partial t} + \Omega_f(z)^2 q - v_d\frac{\partial^3 q}{\partial t\partial z^2} = \frac{A}{D}\frac{\partial v^2}{\partial t^2}, \tag{9}$$

$$\frac{\partial^2 p}{\partial t^2} + \epsilon\Omega_f(z)(p^2-1)\frac{\partial p}{\partial t} + \Omega_f(z)^2 p - v_d\frac{\partial^3 p}{\partial t\partial z^2} = \frac{A}{D}\frac{\partial u^2}{\partial t^2}. \tag{10}$$

where $\Omega_f(z) = 2\pi \mathrm{St} U(z)/D$ is the vortex-shedding angular frequency, and St is the Strouhal number, ϵ and A are dimensionless parameters, and v_d is an effective diffusivity representing the diffusion effect of continuously distributed and interacting van der Pol wake oscillators.

The dimensionless frequency is defined as,

$$\omega_f(z) = \frac{\Omega_f(z)}{\Omega_{ref}} = \frac{U(z)}{U_{ref}}. \tag{11}$$

For uniform sea current, $U(z) = U_{ref}$, $\omega_f(z) = 1$; for linear shear flow, the mean current velocity is chosen as U_{ref}, $U(z) = 2U_{ref}(z/L)$, $\omega_f(z) = 2z$.

2.4 Boundary and initial conditions in dimensionless form

The boundary conditions for the riser in dimensionless form are,

$$v = 0, \quad \frac{\partial^2 v}{\partial z^2} = 0, \quad \text{at} \quad z = 0, v = 0, \quad \frac{\partial^2 v}{\partial z^2} = 0, \quad \text{at} \quad z = 1, \tag{12a,b}$$

$$u = 0, \quad \frac{\partial^2 u}{\partial z^2} = 0, \quad \text{at} \quad z = 0, u = 0, \quad \frac{\partial^2 u}{\partial z^2} = 0, \quad \text{at} \quad z = 1. \tag{12c,d}$$

The initial deflection and velocity of the riser are both considered as zero, with an initial random force. The initial conditions are written as,

$$v(z,0) = 0, \quad \frac{\partial v(z,0)}{\partial t} = 0, \quad q(z,0) = O(10^{-3}), \tag{13a,b,c}$$

$$u(z,0) = 0, \quad \frac{\partial u(z,0)}{\partial t} = 0, \quad p(z,0) = O(10^{-3}). \tag{14a,b,c}$$

3 Integral transform solution

Utilizing the generalized integral transformation method, we derive a set of ordinary differential equations. The specific mathematical manipulations required for this derivation are detailed in a separate paper[14]:

$$\begin{aligned}\frac{d^2\bar{v}_i(t)}{dt^2} + \delta_s \frac{d\bar{v}_i(t)}{dt} + \sum_{j=1}^{\infty}\left(\frac{\gamma}{\mu}A_{ij} + 2\beta\Pi D_{ij}\right)\frac{d\bar{v}_j(t)}{dt} \\ + \left(\beta\Pi^2 - Kc_r^2 - c_\epsilon^2 \sum_{m=1}^{\infty}\sum_{n=1}^{\infty} B_{mn}(\bar{u}_m(t)\bar{u}_n(t) + \bar{v}_m(t)\bar{v}_n(t))\right)\sum_{j=1}^{\infty} P_{ij}\bar{v}_j(t) \\ + c_r^2 \sum_{j=1}^{\infty}(P_{ij} - C_{ij} - D_{ij})\,\bar{v}_j(t) + b^2\alpha_i^4 \bar{v}_i(t) = M_L \sum_{k=1}^{\infty} Q_{ik}\bar{q}_k(t), \quad i = 1,2,3,\ldots,\end{aligned} \tag{15}$$

$$\begin{aligned}\frac{d^2\bar{u}_i(t)}{dt^2} + \delta_s \frac{d\bar{u}_i(t)}{dt} + 2\sum_{j=1}^{\infty}\left(\frac{\gamma}{\mu}A_{ij} + \beta\Pi D_{ij}\right)\frac{d\bar{u}_j(t)}{dt} \\ + \left(\beta\Pi^2 - Kc_r^2 - c_\epsilon^2 \sum_{m=1}^{\infty}\sum_{n=1}^{\infty} B_{mn}(\bar{u}_m(t)\bar{u}_n(t) + \bar{v}_m(t)\bar{v}_n(t))\right)\sum_{j=1}^{\infty} P_{ij}\bar{u}_j(t) \\ + c_r^2 \sum_{j=1}^{\infty}(P_{ij} - C_{ij} - D_{ij})\,\bar{u}_j(t) + b^2\alpha_i^4 \bar{u}_i(t) = M_{DM}H_i + M_{D0}\sum_{k=1}^{\infty} Q_{ik}\bar{p}_k(t), \quad i = 1,2,3,\ldots,\end{aligned} \tag{16}$$

$$\begin{aligned}\frac{d^2\bar{q}_k(t)}{dt^2} + \varepsilon \sum_{l=1}^{\infty}\sum_{r=1}^{\infty}\sum_{s=1}^{\infty} R_{klrs}\bar{q}_l(t)\bar{q}_r(t)\frac{d\bar{q}_s(t)}{dt} - \varepsilon\sum_{j=1}^{\infty} E_{kj}\frac{d\bar{q}_j(t)}{dt} + \sum_{j=1}^{\infty} F_{kj}\bar{q}_j(t) - \nu\sum_{j=1}^{\infty} G_{kj}\frac{d\bar{q}_j(t)}{dt} = A\sum_{i=1}^{\infty} S_{ki}\frac{d^2\bar{v}_i(t)}{dt^2}, \\ k = 1,2,3,\ldots\end{aligned} \tag{17}$$

$$\begin{aligned}\frac{d^2\bar{p}_k(t)}{dt^2} + \varepsilon \sum_{l=1}^{\infty}\sum^{r=1}\sum_{s=1}^{\infty} R_{klrs}\bar{p}_l(t)\bar{p}_r(t)\frac{d\bar{p}_s(t)}{dt} - \varepsilon\sum_{j=1}^{\infty} E_{kj}\frac{d\bar{p}_j(t)}{dt} + \sum_{j=1}^{\infty} F_{kj}\bar{p}_j(t) - \nu\sum_{j=1}^{\infty} G_{kj}\frac{d\bar{p}_j(t)}{dt} = A\sum_{i=1}^{\infty} S_{ki}\frac{d^2\bar{u}_i(t)}{dt^2}, \\ k = 1,2,3,\ldots,\end{aligned} \tag{18}$$

The hybrid analytical numerical solution is implemented by using the software Wolfram Mathematica 13.3.

4 Result

4.1 Model Validation

For the validation part, we select the riser parameters used by Trim et al. (2005) [15]. The empirical values in the wake oscillator equation are set as A = 12 and ϵ = 0.3 Assuming C_{DM} = 1.2, C_{D0} = 0.3, C_{L0} = 0.1, and

St = 0.17. As illustrated in Fig.2, based on the wake oscillator model presented in this paper, the non-dimensional root mean square (RMS) values of the coupled IL and CF VIV under a linear shear flow with a maximum velocity of 0.4 m/s are compared with the experimental results by Trim et al. (2005)[15]. It was observed that the CF responses based on this model closely align with the published results, while the predicted IL response is slightly higher. This discrepancy may be due to some parameters being assumed constant, which in reality vary with environmental changes.

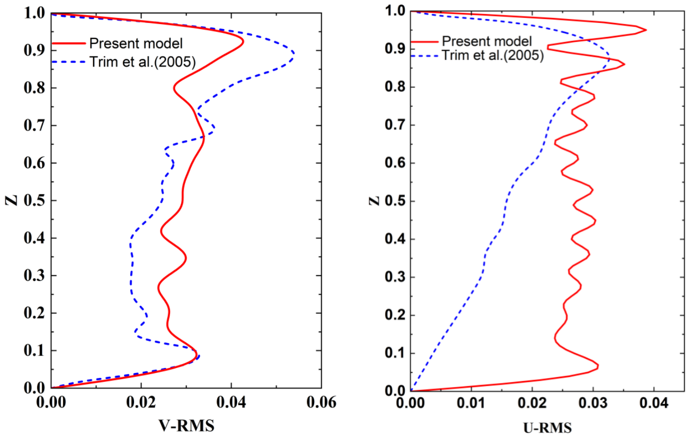

(a) (b)

Figure 2. Comparison of VIV RMS amplitudes for $U_{ref} = 0.4m/s$ in the linear shear flow predicted in the present study and experimental results of Trim et al. (2005), (a) CF direction; (b) IL direction.

4.2 VIV responses of riser

Table 1. Parameters of the riser model

Parameters	Values
Riser Length: L (m)	150
Outer diameter: D (m)	0.25
Inner diameter: d (m)	0.125
Young's modulus: E (Pa)	2.1×10^{11}
Pipe density: ρ_s (kg/m^3)	7800
Internal fluid density: ρ_f (kg/m^3)	8700
Sea water density: ρ_w (kg/m^3)	1020
Top tension coefficient: K_t (-)	2.0
Structural damping coefficient: δ_s (-)	0.005

For the investigation of the dynamic behavior of a fluid-conveying riser, the main parameters of the riser are given in Table1 [10]. The following model parameters are adopted: $C_{DM} = 1.2$, $C_{L0} = 0.3$, $C_{D0} = 0.1$, $St = 0.2$, $A = 12$, and $\varepsilon = 0.3$. The reference current velocity is $U_{ref} = 0.3$ m/s, and dimensionless internal fluid velocities $\Pi = 0$, 0.8 and 1.6. We examine the vibration displacement envelopes of the riser and the contour plots of the vibration displacement to explore the dynamics of coupled VIV.

Fig.3 - Fig.5 illustrate that an increase in non-dimensional internal flow velocity corresponds with a rise in mean displacement, as depicted in the first column. Furthermore, there is a discernible downward shift in the location of the peak mean displacement in the IL direction, transitioning from z=0.55-0.65 at $\Pi = 0$, through z=0.45-0.55 at $\Pi = 0.8$, to z=0.25-0.35 at $\Pi = 1.6$. Examination of the second and fourth columns indicates more vibration modes are activated in both IL and CF directions. Contour plots demonstrate the intensification of traveling wave characteristics in the IL direction, and a transition in vibration mode in the CF direction from standing to traveling waves. It is also observed that the vibration displacement in the IL direction is smaller compared to that in the CF direction. However, the vibration behavior in the IL direction is more complex. In both directions, the vibrations tend to stabilize after the internal flow begins.

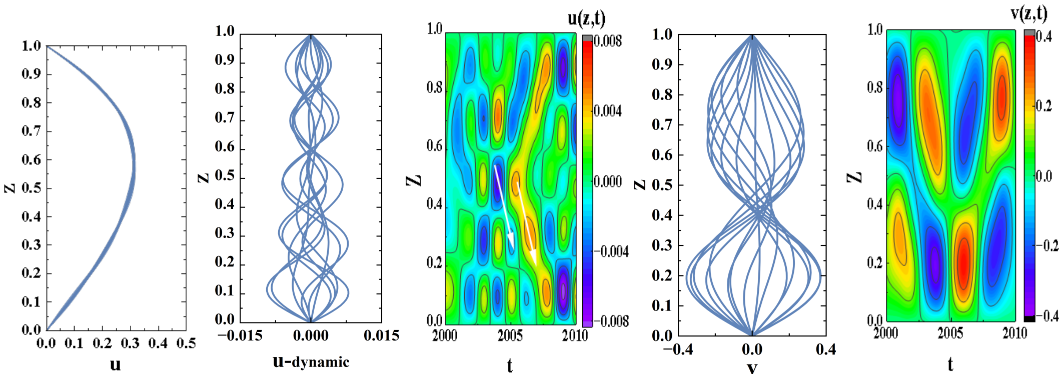

(a) (b) (c) (d) (e)

Figure 3. Vibration displacement responses under linear shear flow with $U_{ref} = 0.3m/s$ and $\Pi = 0$, (a) envelop in IL direction with the mean deflected shape; (b) envelop in IL direction without the mean deflected shape; (c) contour in IL direction; (d) envelop in CF direction; (e) contour in CF direction.

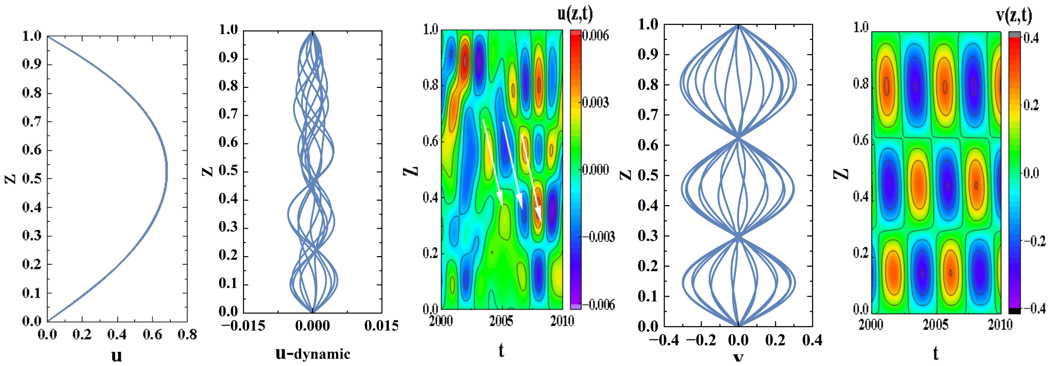

(a) (b) (c) (d) (e)

Figure 4. Vibration displacement responses under linear shear flow with $U_{ref} = 0.3m/s$ and $\Pi = 0.8$, (a) envelop in IL direction with the mean deflected shape; (b) envelop in IL direction without the mean deflected shape; (c) contour in IL direction; (d) envelop in CF direction; (e) contour in CF direction.

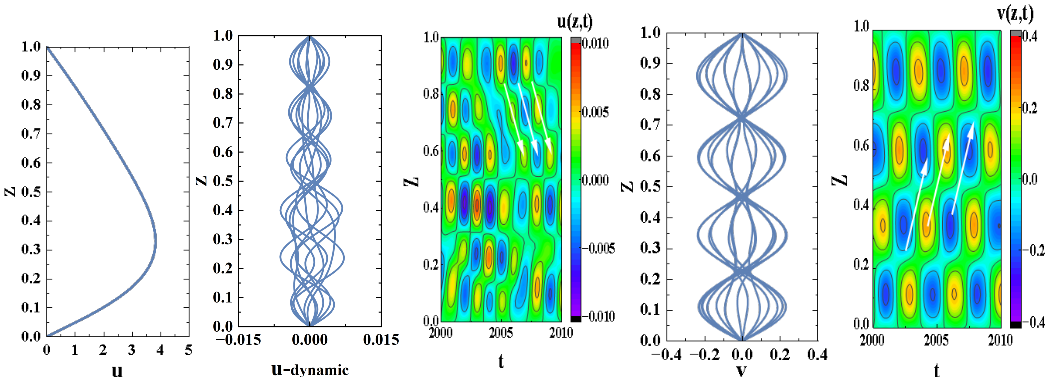

(a) (b) (c) (d) (e)

Figure 5. Vibration displacement responses under linear shear flow with $U_{ref} = 0.3m/s$ and $\Pi = 1.6$, (a) envelop in IL direction with the mean deflected shape; (b) envelop in IL direction without the mean deflected shape; (c) contour in IL direction; (d) envelop in CF direction; (e) contour in CF direction.

5 Conclusions

This paper conducts a study on the coupled IL and CF VIV of a riser that considers both internal and external flow, and considers variable tension and linear shear flow. Structural displacements, standing and traveling wave modes are identified and systematically discussed. Despite the lower amplitude in the IL direction compared to the CF direction, the vibration responses in the IL direction exhibit greater complexity, underscoring the importance of considering the IL direction in the dynamic analysis of the riser. Both internal flow and current velocities significantly influence the IL and CF VIV responses of the riser, in the absence of internal flow, the vibration responses of the riser are unstable, suggesting that a specific ratio of internal to external flow velocities stabilizes the vibration responses of the riser.

Acknowledgements. The authors are grateful for the financial support provided by the Coordenação de Aperfeiçoamento de Pessoal de Nível Superior – Brasil (CAPES), Conselho Nacional de Desenvolvimento Científico e Tecnológico – Brasil (CNPq), FAPERJ, ANP, Embrapii, China National Petroleum Corporation (CNPC), and Young Elite Scientists Sponsorship Program by BAST, Beijing (BYESS2023462).

Authorship statement. The authors hereby confirm that they are the sole liable persons responsible for the authorship of this work, and that all material included herein as part of this paper is either the property (and authorship) of the authors, or has the permission of the owners to be included here.

References

[1] J. Duan, K. Chen, Y. You, and J. Li. Numerical investigation of vortex-induced vibration of a riser with internal flow. *Applied Ocean Research*, vol. 72, pp. 110–121, 2018.

[2] J. Gu, Y. Wang, Y. Zhang, M. Duan, and C. Levi. Analytical solution of mean top tension of long flexible riser in modeling vortex-induced vibrations. *Applied Ocean Research*, vol. 41, pp. 1–8, 2013.

[3] T. Jiang, Z. Liu, H. Dai, L. Wang, and F. He. Nonplanar multi-modal vibrations of fluid-conveying risers under shear cross flows. *Applied Ocean Research*, vol. 88, pp. 187–209, 2019.

[4] G. Gao, X. Cong, Y. Cui, and X. Qiu. Study on vortex-induced vibration of deep-water marine drilling risers in linearly sheared flows in consideration of changing added mass. *Mathematical Problems in Engineering*, vol. 2020, 2020.

[5] P. A. Opinel and N. Srinil. Application of wake oscillators to two-dimensional vortex-induced vibrations of circular cylinders in oscillatory flows. *Journal of Fluids and Structures*, vol. 96, 2020.

[6] M. Gaster. Vortex shedding from slender cones at low reynolds numbers. *Journal of Fluid Mechanics*, vol. 38, n. 3, pp. 565–576, 1969.

[7] R. A. Skop and S. Balasubramanian. A Nonlinear Oscillator Model For Vortex Shedding From A Forced Cylinder Part 2: Shear Flow And Axial Diffusion. *International Journal of Offshore and Polar Engineering*, vol. 5, n. 04, 1995.

[8] M. L. Facchinetti, E. deLangre, and F. Biolley. Vortex shedding modeling using diffusive van der pol oscillators. *Comptes Rendus Mécanique*, vol. 330, n. 7, pp. 451–456, 2002.

[9] L. Mathelin and E. De Langre. Vortex-induced vibrations and waves under shear flow with a wake oscillator model. *European Journal of Mechanics-B/Fluids*, vol. 24, n. 4, pp. 478–490, 2005.

[10] X. Zhang, R. Gou, W. Yang, and X. Chang. Vortex-induced vibration dynamics of a flexible fluid-conveying marine riser subjected to axial harmonic tension. *Journal of the Brazilian Society of Mechanical Sciences and Engineering*, vol. 40, 2018.

[11] Y. He, C. Liu, Y. Yuan, J. Zhao, and J. Su. Vortex-induced vibration of a fluid-conveying riser in shear flow with a diffusive wake oscillator model. In *ISOPE International Ocean and Polar Engineering Conference*, pp. ISOPE–I. ISOPE, 2023.

[12] M. P. Paidoussis. Flow-induced Instabilities of Cylindrical Structures. *Applied Mechanics Reviews*, vol. 40, n. 2, pp. 163–175, 1987.

[13] F. Ge, X. Long, L. Wang, and Y. Hong. Flow-induced vibrations of long circular cylinders modeled by coupled nonlinear oscillators. *Science in China, Series G: Physics, Mechanics and Astronomy*, vol. 52, pp. 1086–1093, 2009.

[14] Z. Li, J. Su, Y. He, C. Liu, Y. Yuan, and J. Zhao. Coupled in-line and cross-flow vortex-induced vibration responses of a variable tension riser in shear flow. In *ISOPE International Ocean and Polar Engineering Conference*, pp. ISOPE–I. ISOPE, 2024.

[15] A. D. Trim, H. Braaten, H. Lie, and M. A. Tognarelli. Experimental investigation of vortex-induced vibration of long marine risers. *Journal of Fluids and Structures*, vol. 21, pp. 335–361, 2005.